Statistical evaluation of clutter filters in color flow imaging

Steinar Bjærum *, Hans Torp

Department of Physiology and Biomedical Engineering, Norwegian University of Science and Technology, N-7489 Trondheim, Norway

Abstract

The filter used to separate blood signals from the tissue clutter signal is an important part of a color flow system. In this paper, statistical detection theory is used to evaluate the quality of the most commonly used clutter filters. The probability of falsely classifying a sample volume as containing blood is kept below a specified threshold. With this constraint, the probability of correctly detecting blood is calculated for all the filters. Using a measured clutter signal, we found that polynomial regression filters and projection-initialized IIR filters are best among the commonly used filters. The probability of correctly detecting blood with velocity 10.1 cm/s was 0.32 for both these filters. The corresponding value for the optimal detector was 0.81, whereas a regression filter that depends on the clutter signal statistics achieved a blood detection probability of 0.72. © 2000 Elsevier Science B.V. All rights reserved.

Keywords: Blood flow; Clutter filters; Doppler; Ultrasound

1. Introduction

In color flow imaging, the signal from blood is much weaker than the signal from tissue. It is therefore difficult to decide if blood is present or not in a given sample volume, especially when imaging small vessels in moving tissue. Commonly used clutter filters to reject the tissue signal are FIR filters, IIR filters with zero-, step-, and projection-initialization, and regression filters. With an efficient clutter filter, the color flow system will reliably detect sample volumes where blood is present. Statistical detection theory can be used to evaluate quantitatively the performance of the different clutter filters, and to find the optimal blood detector. The aim is to maximize the probability of blood detection given a value of the probability of false alarm. It can be shown that, with a Gaussian signal model, the optimal blood detector compares the power at the output of a clutter filter with a threshold. This is a common method used in color flow systems. The optimal clutter filter depends on both the clutter and blood signal statistics and is difficult to implement in practice. In this study we compare the blood detection performance of the different clutter filters with each other and with the optimal filter. In vivo digital RF data are used to calculate the statistics

for the tissue signal, and a theoretical signal model is used for the blood. In this way the performance of the different filters is evaluated in different imaging situations.

2. Signal model

The signal vector x is the complex demodulated Doppler signal from a single sample volume and consists of N temporal samples. It is a zero mean complex Gaussian process with three independent components: clutter, white noise, and blood. The signal is characterized by the correlation matrix R_x, which is given by

$$R_x = R_c + \sigma_n^2 I + R_b, \tag{1}$$

where R_c is the clutter correlation matrix, σ_n^2 is the noise variance, I is the identity matrix, and R_b is the blood correlation matrix.

3. Clutter filters

A general linear filter is described by a matrix multiplication of the signal vector, $y = Ax$. The matrix rows are a set of (possibly) different FIR filters for each time instant. With a time variant filter, a frequency response function $H_2(\omega)$ can be defined as the power of the

* Corresponding author. Fax: +47-735-98613.
E-mail address: steinarb@medisin.ntnu.no (S. Bjærum)

output signal when the input is a complex harmonic signal:

$$H_2(\omega) = \frac{1}{N}(Ae_\omega)^{*T}Ae_\omega = \frac{1}{N}\|Ae_\omega\|^2, \qquad (2)$$

where $e_\omega = [1\ e^{i\omega}\ \cdots\ e^{i(N-1)\omega}]^T$ is a vector of N samples of a complex sinusoid, and $(Ae_\omega)^{*T}$ means that the vector is complex conjugated and transposed. To get a well-defined frequency response for a real valued signal, an ensemble average over all possible phases is necessary, as described in Ref. [1].

3.1. FIR filters

FIR filters are described by the transfer function $H(z) = \Sigma_{k=0}^{M} b_k z^{-k}$, where M is the filter order. It is possible for FIR filters to have a linear phase response by imposing symmetry constraints on the impulse response [2], but for the same order a better amplitude response can be obtained by discarding the phase. The linear phase FIR filters considered in this paper were designed using the McClellan–Parks algorithm [2]. The minimum phase FIR filters were designed by factorization of a linear phase filter of order $2M$ as described in Ref. [3].

The signal consists of N samples, but the first M output samples must be discarded since the output is not valid until the input data reach all the filter registers. This means that only $N-M$ samples are available for estimating flow parameters, resulting in increased estimator variance. The FIR filter can be formulated as an $(N-M) \times N$ matrix with a time-shifted version of the impulse response in each row. For FIR filters, the frequency response defined in Eq. (2) is equal to the squared magnitude of the Fourier transform of the impulse response, $H_2(\omega) = |H(\omega)|^2$.

The frequency responses of linear- and minimum-phase FIR filters of order five in Fig. 1 show that the
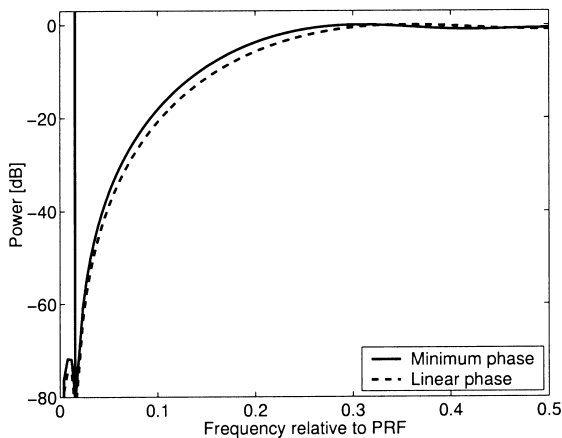

Fig. 1. Frequency responses of fifth-order FIR filters. The vertical line indicates the experimental clutter velocity.

minimum phase filter has the steepest transition region. It is advantageous with a filter zero at zero frequency since this removes the mean value of the signal, and thus the signal from stationary tissue. This is accomplished by a filter of odd order.

3.2. IIR filters

IIR filters have both zeros and poles, and are described by the transfer function $H(z) = \Sigma_{k=0}^{K} b_k z^{-k} / \Sigma_{k=0}^{K} a_k z^{-k}$, where K is the filter order. Because of the poles, the output consists of a transient signal in addition to the steady state signal. In Ref. [4] a matrix formulation of an IIR filter is developed:

$$y = Cv(0) + Dx, \qquad (3)$$

where $v(0)$ is a vector containing the initial values of the K filter registers. The goal of filter initialization is to choose a value of $v(0)$ that minimizes the transient response. Three different initialization techniques are considered below.

3.2.1. Zero initialization
The filter registers are simply set to zero, $v(0) = 0$.

3.2.2. Step initialization
The input signal is assumed to have a constant value equal to the first signal sample $x(0)$. The transient for such a signal is suppressed by setting $v(0) = x(0) v_{step}(\infty)$, where $v_{step}(\infty)$ is the filter state an infinitely long time after a unit step is applied at the input.

3.2.3. Projection initialization
By setting $v(0) = -(C^T C)^{-1} C^T Dx$, the output of the projection initialized IIR filter is given by $y = [I - C(C^T C)^{-1} C^T]Dx$. The matrix $C(C^T C)^{-1} C^T$ is recognized as the projection into the range of the matrix C, and thus into the K-dimensional subspace containing the transient response [4]. The output of the filter is thus the projection of the steady state response into the orthogonal complement of the transient subspace. In addition to removing the transient signal, the component of the steady state response in the transient subspace is removed.

The frequency response of a fourth-order Chebyshev filter with the different initializations applied to a signal vector of length $N = 9$ is shown in Fig. 2 For this short signal length only the projection initialization results in a sufficient stopband width, but the transition band is much wider than expected from the steady state response. The transient dies out with time, but, for this short signal, no significant improvement was obtained by discarding the first samples.
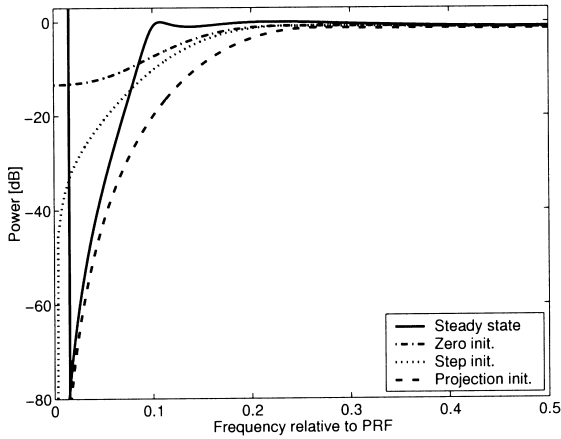
Fig. 2. Frequency responses of a fourth-order Chebyshev filter with different initializations. The signal vector length is $N=9$, and the 1 dB cut-off frequency of the steady state response is 0.1. The vertical line indicates the experimental clutter velocity.

3.3. Regression filters

A regression filter calculates the best least squares fit of the signal to a set of curveforms modeling the clutter space, and subtracts this clutter approximation from the original signal. The curveforms span a subspace of the N-dimensional signal space that we call the clutter space. The regression filter matrix is given by $A = I - P$, where P is a projection matrix into the clutter space. In a polynomial regression filter of order K, the polynomials of order zero to K are used as a basis for a $K+1$-dimensional clutter space [5].

The output vector of both regression filters and projection-initialized IIR filters is contained in a subspace of the N-dimensional vector space. This results in very similar frequency responses, as observed by comparing the response of the third-order polynomial regression filter (four-dimensional clutter space) in Fig. 3 with
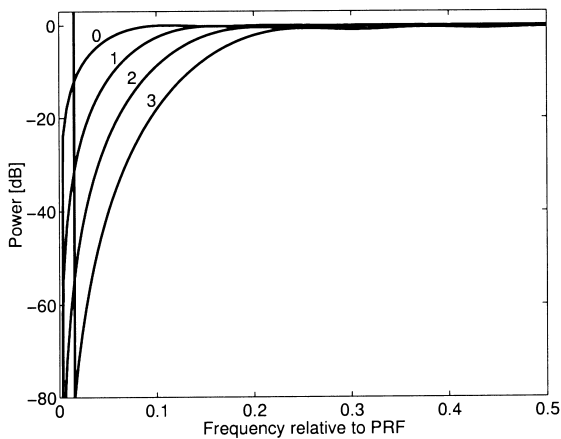

Fig. 3. Frequency responses of polynomial regression filters of order 0–3 with signal vector length $N=9$. The vertical line indicates the experimental clutter velocity.

the response of the projection-initialized IIR filter in Fig. 2.

3.4. An adaptive regression filter

A more efficient clutter filter is obtained by using a filter matrix that depends on the clutter signal statistics [6]. This filter is based on the discrete Karhunen–Loève transform (DKLT) [7], which is a generalization of the discrete Fourier transform for random signals. The DKLT is a signal expansion using the eigenvectors of the correlation matrix as basis vectors. In the adaptive regression filter, the eigenvectors of R_c corresponding to the K largest eigenvalues are used as a basis for the clutter space. This filter is optimal in the sense that, for a given order K, it removes the best statistical mean square approximation of the clutter signal.

4. Detection of blood

In the blood detection problem a decision rule for each sample volume is sought to decide which of the hypotheses

$$H_0: \text{no blood is present} \quad H_1: \text{blood is present} \quad (4)$$

is true. The observed vector is complex Gaussian under both hypotheses, but with different correlation matrices

$$R_{x|H_0} = R_c + \sigma_n^2 I$$
$$R_{x|H_1} = R_c + \sigma_n^2 I + R_b = R_{x|H_0} + R_b. \quad (5)$$

The detector is characterized by the probability of false alarm P_F and the probability of detection P_D defined by

$$P_F = P(\text{choose } H_1 | H_0 \text{ is true})$$
$$P_D = P(\text{choose } H_1 | H_1 \text{ is true}). \quad (6)$$

The assumption in the development of the optimal detector is that the probability density function of the observation vector, $p_{x|H_i}$, is known under both H_0 and H_1. In this case the Neyman–Pearson lemma [8] tells us that P_D is maximized under the constraint $P_F \le \alpha$ by a likelihood ratio test [LRT, $L(x)$] given by

$$L(x) = \frac{p_{x|H_1}(x|H_1)}{p_{x|H_0}(x|H_0)} \underset{H_0}{\overset{H_1}{\gtrless}} \gamma. \quad (7)$$

The Bayes theory of hypothesis testing also leads to the LRT in Eq. (8). In Ref. [9] the LRT is simplified to

$$l(x) = \| [I - (I + \Lambda)^{-1}]^{1/2} E^{*T} x \|^2 \underset{H_0}{\overset{H_1}{\gtrless}} \eta, \quad (8)$$

where $l(x)$ is a sufficient statistic of the test in Eq. (7), and E and Λ solves the generalized eigenvalue problem $R_b E = R_{x|H_0} E \Lambda$. Eq. (8) shows that the optimal detector passes the signal through a signal-dependent filter, and

compares the power of the filtered signal to a threshold. Conventional color flow systems have the same structure, but with a suboptimal filter matrix. The probabilities of detection and false alarm can be calculated as described in Ref. [9] and used to compare the detector performance of the different filters.

5. Experimental results

5.1. Data acquisition

To evaluate the detectors, digital RF data were recorded using a GE Vingmed Ultrasound System Five ultrasound scanner with a linear array transducer. The data were recorded from the thyroid gland with substantial probe movement during the recording. The scanner was set up with center frequency 5.7 MHz, pulse length 0.525 μs, radial sampling frequency 2 MHz, nine temporal samples in each sample volume, and pulse repetition frequency 5 kHz, giving a Nyquist velocity of 34 cm/s. The digital data were stored as complex baseband signals where the in-phase and quadrature signal samples were represented as 16 bit integers. This data were transferred from the scanner and processed on a standard computer using MATLAB.

An estimate of $R_{x|H_0}$ was found by spatial averaging in a region with approximately constant clutter properties. The white noise power σ_n^2 was estimated by averaging the three smallest eigenvalues of $R_{x|H_0}$, resulting in an estimated clutter to white noise ratio of 52 dB. The mean tissue movement was estimated to 1.0 cm/s. The signal from blood was modeled as a single frequency signal, specified by the blood velocity and power. The blood signal to white noise ratio was set to 6 dB in all the calculations.

5.2. Filter performance

The filter performances are summarized in Table 1. The probability of false alarm is kept constant at $P_F = 0.05$, and the probability of detection P_D is calcu-

lated for the different filters and different blood velocities. As expected, the performance improves with increased blood velocity for all the filters. For our clutter signal, the step-initialized IIR filter has poor performance for all the blood velocities. The clutter is not sufficiently rejected, as can be explained by the narrow stopband for step initialization seen in Fig. 2. There was no significant increase in the -40 dB stopband width for step initialization by increasing the steady state cutoff frequency and/or the filter order. An improvement is expected by increasing the number of signal samples, but even for 32 signal samples the stopband is very narrow, as shown in Ref. [4]. Only narrowband clutter signals can thus be sufficiently rejected by step-initialized IIR filters. The FIR filters have poor performance for low velocities. The polynomial regression filter and the projection-initialized IIR filter have similar performances and are best among the non-adaptive filters for low velocities. For higher velocities, the FIR filters are slightly better. For all the non-adaptive filters there is a slight variation in P_D for large velocities. This variation seems to coincide with the passband ripple. The adaptive regression filter has an overall higher P_D than any of the non-adaptive filters, with a very large improvement for the lowest blood velocities.

6. Conclusions

Among the non-adaptive clutter filters, the projection initialized IIR and polynomial regression filters provide the largest overall probability of blood detection. FIR filters are inferior for low blood velocities, with a small improvement by allowing non-linear phase. For IIR filters, projection initialization was the only initialization scheme resulting in reliable blood detection with the measured clutter signal. However, owing to the initialization, there is no longer any computational advantage in using an IIR filter compared with a regression filter. The adaptive regression filter is relatively close to the optimum detector. In the given clutter conditions it is

Table 1
Probability of detection P_D for different filters and blood velocities. The probability of false alarm is kept constant at $P_F = 0.05$

Velocity (cm/s)	P_D						
	Optimal	Adap. regression	Poly. regression	Proj. init. IIR	Step init. IIR	FIR min. phase	FIR lin. phase
6.8	0.50	0.34	0.07	0.07	0.05	0.06	0.06
10.1	0.81	0.72	0.32	0.32	0.05	0.23	0.16
13.5	0.88	0.81	0.65	0.65	0.05	0.57	0.49
16.9	0.90	0.81	0.74	0.74	0.05	0.73	0.70
20.3	0.92	0.82	0.73	0.72	0.05	0.77	0.77
23.7	0.92	0.82	0.75	0.73	0.05	0.75	0.80
27.0	0.92	0.82	0.75	0.74	0.05	0.72	0.79
30.4	0.92	0.83	0.75	0.73	0.05	0.73	0.77

the only filter able to detect blood with velocity 10 cm/s, but at a very high computational cost.

References

[1] H. Torp, Clutter rejection filters in color flow imaging: a theoretical approach, IEEE Trans. Ultrason. Ferroelectr. Freq. Contr. 44 (1997) 417–424.

[2] J.G. Proakis, D.G. Manolakis, Digital Signal Processing, Principles, Algorithms, and Applications, second ed.Macmillan, New York, 1992.

[3] J.S. Lim, A.V. Oppenheim (Eds.), Advanced Topics in Signal Processing, entice Hall, Englewood Cliffs, NJ, 1988.

[4] E.S. Chornoboy, Initialization for improved IIR filter performance, IEEE Trans. Signal Process. 40 (1992) 543–550.

[5] A.P.G. Hoeks, J.J.W. van de Vorst, A. Dabekaussen, P.J. Brands, R.S. Reneman, An efficient algorithm to remove low frequency Doppler signals in digital Doppler systems, Ultrason. Imag. 13 (1991) 135–144.

[6] S. Bjærum, H. Torp, Optimal adaptive clutter filtering in color flow imaging, Proc. IEEE Ultrason. Symp. 2 (1997) 1223–1226.

[7] C.W. Therrien, Discrete Random Signals and Statistical Signal Processing, Prentice Hall, Englewood Cliffs, NJ, 1992.

[8] H.L. Van Trees, Detection, Estimation, and Modulation Theory, vol. 1, Wiley, 1968.

[9] S. Bjærum, H. Torp, Blood detection performance in moving tissue, Proc. IEEE Ultrason. Symp. 2 (1998) 1571–1574.